

Correlative Postural Gait Descriptor to Discriminate Parkinsonian Findings in a Markerless Analysis

Análisis de patrones parkinsonianos de la marcha usando descriptores correlativos a partir de mecanismos sin marcadores

 Jean Portilla¹;  Edgar Rangel Pieschacon¹;  Odair Bacca¹;  Paula C. Ramírez¹;  Luis Guayacán¹;
  Fabio Martínez Carrillo¹

¹Universidad Industrial de Santander, Bucaramanga, Colombia

Correspondence: famarcar@saber.uis.edu.co

Received: 13 March 2025

Accepted: 20 January 2026

Available: 12 February 2026

How to cite / Cómo citar

J. Portilla, E. Rangel Pieschacon, O. Bacca, P. C. Ramírez, L. Guayacán, and F. Martínez Carrillo, "Correlative Postural Gait Descriptor to Discriminate Parkinsonian Findings in a Markerless Analysis," *Tecnológicas*, vol. 29, no. 65, e3432, 2026. <https://doi.org/10.22430/22565337.3432>



Abstract

Parkinson's disease (PD) is one of the most prevalent neurodegenerative disorders worldwide, with over 10 million cases reported globally. Currently, gait analysis is crucial for quantifying motor abnormalities, and most methods rely on physical markers, which alter patients' natural movements and have limitations in explaining spatiotemporal relationships of the joints. This study aimed to implement a markerless methodology that reconstructs gait postures and encodes spatiotemporal joint information as covariance descriptors, which are then used to discriminate between subjects with Parkinson's disease and healthy controls. The methodology consisted of a study of covariance encoding of postures and joint trajectories to identify potential coordination patterns that aid in PD classification. The results obtained in a population of 30 subjects, recorded in a total of 240 videos, approved by the Scientific Research Ethics Committee of Universidad Industrial de Santander (CEINCI), showed an average PD classification accuracy of 75% and an AUC of 74%. In conclusion, the correlation descriptors demonstrated the potential to discriminate between subjects with PD and healthy controls and to encode coordination patterns. Furthermore, the visual correlation maps show differences between the two groups, which can further support routine clinical analysis.

Keywords

Correlation matrices, covariance matrices, gait analysis, motion capture, Parkinson disease.

Resumen

La enfermedad de Parkinson (EP) es uno de los trastornos neurodegenerativos más prevalentes en todo el mundo, con más de 10 millones de casos reportados a nivel mundial. Hoy en día, el análisis de la marcha es crucial para cuantificar anomalías motoras y en gran parte se basan en marcadores físicos, alterando los gestos naturales de los pacientes, con limitaciones para explicar las relaciones articulares espaciotemporales. Este trabajo tuvo como objetivo implementar una metodología sin marcadores físicos que recupera posturas de locomoción de la marcha y codificar información articular espaciotemporal como descriptores de covarianza, que se utilizan además para obtener discriminación entre sujetos con Parkinson y sujetos de control. La metodología empleada consistió en un estudio de codificación de covarianzas de posturas y trayectorias articulares para explicar posibles patrones de coordinación que benefician la clasificación de la EP. Los resultados obtenidos en una población de 30 sujetos, grabados en un total de 240 videos, avalado por el comité de ética en investigación científica de la Universidad Industrial de Santander (CEINCI), el enfoque propuesto fueron una clasificación de precisión de EP promedio del 75 % y un AUC del 74 %. Finalmente se concluye que los descriptores correlativos evidenciaron la capacidad potencial de discriminar sujetos con EP y codificar patrones de coordinación. Además, los mapas correlativos visuales muestran diferencias entre poblaciones, lo que puede respaldar aún más el análisis de rutina clínica.

Palabras clave

Matrices de correlación, matrices de covarianza, análisis de la marcha, captura de movimiento, enfermedad de Parkinson.

1. INTRODUCTION

Parkinson's disease (PD) is the second most prevalent neurodegenerative disorder worldwide, according to the World Health Organization [1]. Globally, over 10 million cases were reported in 2023 [2], and it is estimated that more than 12 million people will be affected in 2040 [3]. The diagnosis of this disease is mainly based on motor symptoms evaluation [4]. Gait observational analysis is a primary tool to diagnose PD, to plan treatments, and establish a prognosis [5]. During such examinations, experts typically look for common PD patterns such as coordination of movements between parts, bradykinesia, rigidity, tremors, loss of balance.

PD currently has no cure, and no definitive biomarker exists for its diagnosis or progression follow-up. Even worse, PD is multifactorial, presenting motor and non-motor symptoms that vary in detection time, magnitude, and occurrence. Gait, a complex process that involves coordinated movements, is crucial for characterizing PD motor symptoms, supporting early detection and disease monitoring [6], [7]. The gait analysis provides objective metrics to assess motor function, characterizing motor disturbances such as tremors, postural instability, and locomotion disturbances [6], [8]. For instance, the PD manifests gait with short steps and bradykinesia expressed as reduced spontaneous gestures, and decreased arm swing while walking [9]. Rigidity is a symptom observed in passive patient movements, both for flexor and extensor muscles. This condition is often described as "cogwheel rigidity" due to the sensation of catching or jumping when passively moving joints [10]. In a study of 136 patients, 80% exhibited such patterns [11].

Marker-based systems quantify joint trajectories and postural behaviors, providing a valuable tool to assess motor alterations [12]. These systems place markers near joints, capturing their trajectories during controlled locomotion. A biomechanical model then establishes body dynamics and joint relationships to detect gait abnormalities. However, they alter natural movement and often focus on isolated limbs, limiting their scope for parkinsonism patterns. Markerless computer vision alternatives analyze videos and compute descriptors to correlate PD observations [13]. These methods classify video inputs and offer promising diagnostic support. However, they are sensitive to scene artifacts (e.g., brightness changes, background motion), which may introduce non-clinical patterns and reduce anatomical and gait-related information. Consequently, their performance may be limited in clinical scenarios that are different from the training data.

PD-related motor alterations are analyzed through sensors measuring kinematic parameters [14], [15]. Electrogoniometers and gyroscopes capture joint angles and velocities, while inertial sensors measure linear or angular accelerations [16]. Also, marker-based methodologies track foot trajectories for classification using decision trees and SVM [17]. Optical marker-based systems

extract gait features like step length and foot angle but face geometric constraints [5]. These sensor-based setups depend on precise sensor placement, complex protocols, and feasibility constraints, altering natural movement and requiring specialized personnel [18], [19].

Recently, machine learning and deep learning have been applied to PD motor tracking [13]. PD gait features extracted from videos have been mapped to classifiers for patient discrimination [20]. Kinect-based approaches collect skeleton data but are limited to indoor infrared-based analysis [21]. Pose estimation enables markerless gait analysis, computing knee angles from 2D postures [22], though often limited to local angle descriptions. CNN-based models classify gait disorders from human posture estimation but lack a comprehensive patient video analysis [23]. Computer vision methods [24] employed 3D convolutional networks to identify PD gait patterns into a 22 subject's dataset [25]. Through backpropagation, characteristic PD gait features were highlighted, distinguishing them from normal gait [23]. However, this approach provides a global characterization, defining regions instead of analyzing individual limb movements, which may limit its clinical applicability.

In this context, the objective of this work was to introduce a markerless methodology that recovers postures during gait locomotion exercise and represents kinematic information using coded covariance descriptors, with the capability to explain and discriminate coordination anomaly patterns associated with Parkinson's disease. First, we computed joint trajectories and carried out a correlation analysis of the entire body to define potential patterns to Parkinson's. For doing so, we built covariance matrices that summarize the dynamic of each joint trajectory and allow a coordination study of postural structure. The resultant covariance matrices are projected to supervise machine learning algorithms to obtain a Parkinson classification, regarding population control. Also, these covariance descriptors expose observational patterns that fully explain abnormal behaviors during locomotion. These features are predominant in clinical practice, for instance, to determine the coordination capability of subjects.

2. PROPOSED APPROACH

This work introduces a new covariance descriptor with the capability to recover coordination-associated gait patterns, computed from joint correlations during a walking exercise. To do so, markerless joint trajectories are computed from an OpenPose generator [26]. Let k represent the number of the patient's video, K the maximum number of videos, n the current frame, N the total number of frames, j the joint, and J the total number of joints. The coordinate of each joint is denoted by X . Then, a covariance descriptor summarizes kinematic coordination patterns, with the capability to classify Parkinsonian patterns. These second-order patterns are represented in correlation matrices, capable of explaining abnormalities and offering support during clinical analysis. Additionally, the covariance descriptors are projected onto supervised classifiers to estimate PD probability and classification. The pipeline of the proposed approach is summarized in Figure 1.

2.1 Gait Data

This study includes a balanced dataset of 14 individuals with PD (age: 73 ± 7.45 years, 11 male) and 16 healthy controls (age: 70.4 ± 5.38 years, 8 male). PD participants were in disease severity stages 1 to 3 on the Hoehn and Yahr scale [27]. Each subject performed eight walking trials (4 right and left sagittal walks and 4 left and right sagittal walks) with their own walking shoes, at a comfortable speed along a 3-meter path analyzed in camera, resulting in 240 video sequences. Recordings were captured in the sagittal plane at 60 fps (1920x1080 resolution) using a Nikon 3500 camera, without restrictions on clothing or gait development. The large number of repetitions helps to prevent patients from concealing symptoms in the initial videos, while the later recordings are expected to exhibit more natural movements, possibly with a slight level of fatigue.

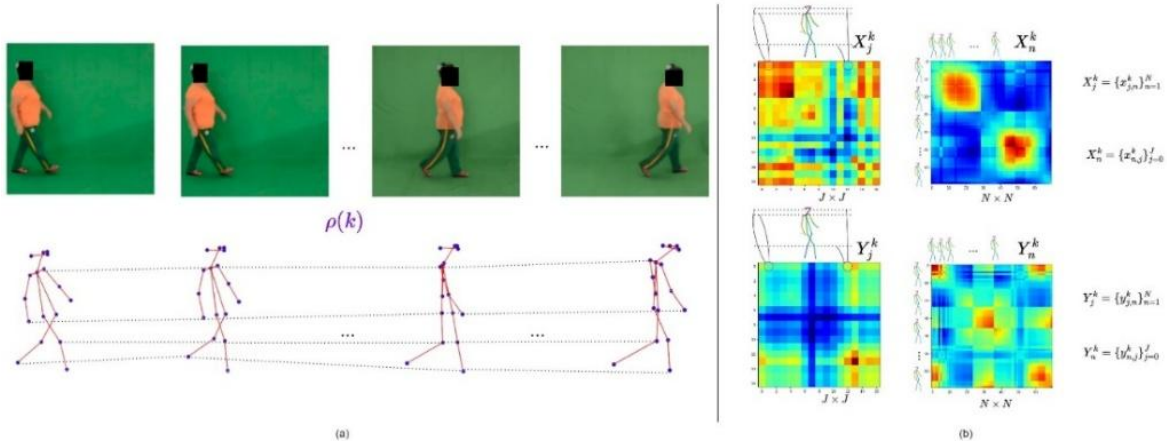


Figure 1. (a) Selection of patient gait videos. Posture extraction, capturing 2D coordinates of patient joints in each frame. (b) Collection of covariance matrices for movement characterization between joints and poses. Source: own elaboration.

Confounding variables were analyzed using logistic regression, evaluating gender and age. Odds ratios were 9.38 (crude) and 8.13 (adjusted), with $p < 0.05$, indicating no significant confounding effects on gait analysis. The dataset ensures realistic motion capture, where later trials may exhibit more natural movement and slight fatigue. All participants provided informed consent, and the study received ethical approval.

Since covariance measures represent global second-order statistics primarily reflecting temporal variations, it was not necessary to include information like height or segmental physical dimensions in the analysis. Moreover, anthropometric information of this kind was not available in the present study.

This data collection was approved by the Scientific Research Ethics Committee of the Universidad Industrial de Santander (CEINCI) with approval code of 4110, under the ethical clearance for the project "Characterization of abnormal movements in Parkinson's disease from oculomotor and gait patterns through multimodal approaches based on computer vision." The study was supported by the external call from MINCIENCIAS under the framework of the 2022 ECOS-Nord Academic Mobility Program (Call No. 923). Documentation of the ethics approval is provided as supplementary material.

2.2 Markerless pose generation

We utilized OpenPose, a widely used pose estimator effective for sagittal-plane postural recovery [26]. In Figure 2, explains the final activations from these fields, which serve as intermediate locomotion process representation. In contrast, the Joint Confidence Maps $S = \{S_j\}$; $S_j \in \mathbb{R}^{w \times h}$ recovers probability maps for the position of a particular body part j . Similarly to the generation of Part Affinity Fields (L), a dedicated network ρ computes S from the features F at the first-time step as: $S^1 = \rho_1(F)$. Then, a refinement is achieved as follows: $S_t = \rho(L_{t-1}, F, S_{t-1})$.

These S maps may also represent a potential intermediate gait representation that encodes positional joint maps during walking. Once the T refinement stages have been completed, the candidate parts are assembled using a bipartite graph matching process. A bipartite graph is created where the graph nodes represent detection candidates for j_1 and j_2 , and the graph edges represent all possible connections between these candidates, with each edge weighted by the probability that the candidates are related. The objective is to find a matching in the bipartite graph that maximizes the total weight of the selected edges. This matching ensures that each detection candidate for j_1 is associated with exactly one detection candidate for j_2 , and vice versa. As a result, the connection of different body parts with spatial and anatomical meaning is obtained (see an example in Figure 2).

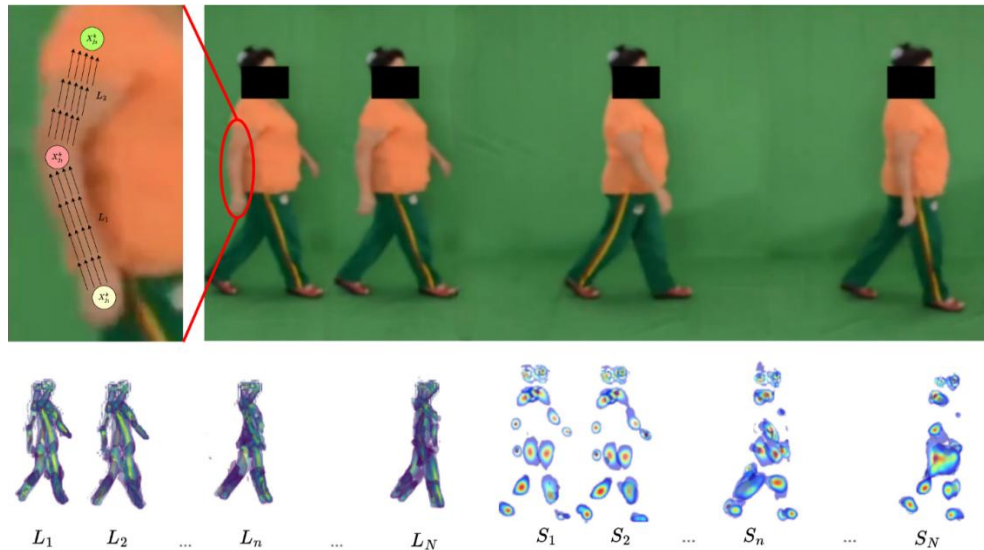


Figure 2. Extraction process of postures using affinity fields (L) and confidence maps (S) in OpenPose. Source: own elaboration.

The Part Affinity Fields (L) are 2D vector maps ($L = \{L_i\}; L_i \in R^{w \times h \times 2}$) encode the orientation and magnitude of connections between body joints, modeling spatial and anatomical relationships (Figure 2). They are iteratively refined as: $L_t = \varphi(L_{t-1}, F, S_{t-1})$. Also, the Joint Confidence Maps (S) are probability maps ($S = \{S_j\}; S_j \in R^{w \times h}$) that estimate the likelihood of each joint's position. Their refinement is defined as $S_t = \rho(L_{t-1}, F, S_{t-1})$.

At the end of processing, OpenPose assembles detected joints into complete poses using bipartite graph matching. The graph nodes represent joint candidates j_1 and j_2 , while edges encode connection probabilities. The optimal matching maximizes total edge weight, ensuring spatially and anatomically meaningful connections (Figure 2). Furthermore, the generation of joints is performed independently, without relying on a predefined centroid, allowing the reconstruction of human poses based solely on local joint relationships rather than a central reference point.

2.3 Gait descriptor from second-order matrices

Human gait results from the interaction of bodily subsystems enabling coordinated movement. Variability in these subsystems, such as dopamine deficits, can affect adaptability and control of locomotion. Gait correlation indexes help explain motor impairments by assessing coordination levels required for efficient movement [28]. We propose a gait descriptor based on postural relationships during walking, capturing correlations among joint trajectories and summarizing them into a second-order matrix descriptor. This descriptor is mapped to machine learning classifiers to distinguish Parkinson's disease (PD) from control populations. The covariance matrix for a video with N frames is computed as (1).

$$\Sigma(j_1, j_2) = \frac{1}{N - 1} \sum_{n=1}^N (X_{n,j_1} - \bar{X}_{j_1})(X_{n,j_2} - \bar{X}_{j_2}) \tag{1}$$

Where $X_{n,j}$ is the position of joint j at frame n , and \bar{X}_j is its mean position across frames. This representation serves as both a compact descriptor of motor coordination and an explainable tool for medical experts. The covariance matrix can be normalized into a correlation matrix represented in (2).

$$\text{Corr}(j_1, j_2) = \frac{\Sigma(j_1, j_2)}{\sqrt{\Sigma(j_1, j_1)\Sigma(j_2, j_2)}} \quad (2)$$

Bounded between -1 and 1, where 0 indicates no linear dependency between joint trajectories. To analyze PD symptoms, we explore descriptors: one using only upper-limb joints, and another using lower-limb joints. These versions allow us to describe symptoms such as postural instability of the trunk, upper limb movement, or the capacity to walk effectively through synchronized movements. Alternatively, we computed postural correlations during locomotion to recover global coordination patterns of joints J across the N video frames. In this analysis, we assess the positional behavior in the X-axis of each of the J joints in each of the N frames.

Since covariance descriptors often contain redundant correlations, we perform spectral decomposition to extract the first k eigenvectors of $\Sigma(j_1, j_2)$, forming a matrix $V \in \mathbb{R}^{J \times k}$. The reduced covariance matrix is represented in (3).

$$\Sigma_r = V\Lambda V^T \quad (3)$$

Where Λ contains the largest eigenvalues. These eigenvectors highlight key motion variations, aiding in PD characterization [29]. This process enhances discrimination by eliminating redundancy and emphasizing relevant coordination patterns.

2.4 PD classification

To classify Parkinsonian gait, we projected covariance descriptors of joint trajectories into five machine learning models: Random Forest (RF), Support Vector Machine (SVM), K-Nearest Neighbors (KNN), Gaussian Naive Bayes (NB), and Gradient Boosting (GB). The classifiers are described as follows:

- Random Forest (RF): A non-parametric classifier that constructs trees based on covariance matrices of joint coordinates. The final prediction is obtained via majority voting among trees, leveraging their diversity for robust classification [30].
- Support Vector Machine (SVM): A kernel-based method that defines classification boundaries using support vectors. We employed a linear kernel to evaluate the descriptor's effectiveness in distinguishing Parkinson's from control groups. The optimization problem is defined as in (4).

$$\min \frac{1}{2} \|w\|^2 \text{ s.t. } y_i(w \cdot x_i + b) \geq 1, \forall i = 1, \dots, N \quad (4)$$

Where y_i is the class label, x_i the covariance matrix, and N the number of samples.

- K-Nearest Neighbors (KNN): A non-parametric classifier that assigns labels based on the majority vote of the k -nearest neighbors, using Euclidean distance among covariance matrices [31]. The value of k was set as the square root of the training dataset size.
- Gaussian Naive Bayes (NB): A probabilistic classifier assuming Gaussian-distributed features, computing the posterior probability as defined as in (5).

$$P(C|X) \propto P(C) \prod_i P(X_i|C) \quad (5)$$

Where C represents the class (Parkinson's or Control) [32].

- Gradient Boosting (GB): An iterative algorithm that optimizes a loss function by combining weak decision trees, as shown in (6).

$$F(x) = \sum_{m=0}^M \rho_m h_m(x) \quad (6)$$

Where ρ_m is the weight of the m -th tree. Regularization constraints such as tree depth help prevent overfitting [33].

2.5 Experimental setup

From each video, we resized the spatial dimension size to $95 \times 95 (h \times w)$ and selected $N = 70$ intermediate frames that represent around one or two gait cycles. In each video recording, a complete gait cycle is ensured, guaranteeing a comprehensive exposure of kinematics during locomotion. Each frame was individually passed through OpenPose network, using the 10 first layers of VGG19 model with a number of stages t set to 6, generating Part Affinity Fields (L) and Joint Confidence Maps (S) with enough pose information. In this work, the pose P comprises 18 key articulation points ($|J| = 18$). A cross-validation was conducted under a leave-one-patient-out scheme, using iteratively, one patient for test while the remaining patients were used for training the models. This process will be applied to each patient, and standard classification metrics were calculated, namely, the accuracy, the AUC, the recall. Covariance matrices were constructed from sizes of 17×17 (among joint trajectories) and 70×70 (among pose frames), respectively. Also, a spectral analysis was carried out with reduced covariance descriptors, recovering most significant eigenvectors from higher associated eigenvalues. For pose-frame covariances were analyzed with reduced sizes of [10, 20, 30, 40, 50, 60].

All classifiers were implemented using the scikit-learn library with empirically fixed hyperparameters, without applying nested validation or hyperparameter search, as the main objective was to compare covariance-based descriptors under identical training conditions. The selected configurations followed standard defaults or prior literature in gait classification: Gradient Boosting with a number of estimators 100, a learning rate of 0.1, and a maximum depth of 3, Random Forest with a number of estimators of 100, without a maximum depth, and bootstrap activated, K-Nearest Neighbors with a number of neighbors of 5, Support Vector Machine with a radial basis function (RBF) kernel, using a regularization parameter C of 1.0 and gamma set to scale, and Gaussian Naïve Bayes. Model evaluation was performed using a Leave-One-Patient-Out (LOPO) cross-validation strategy, ensuring that each patient was excluded from training and used solely for testing to guarantee strict subject-independent validation.

3. EVALUATION AND RESULTS

We conducted an initial evaluation to measure the capability of covariance descriptors, coding only coordinate joint positions, independently (size of 17×17). Such a covariance descriptor was projected onto various typical machine learning classifiers to obtain a Parkinson's characterization measure, including a confidence interval (IC) of 95%. Table 1 summarizes the results obtained with these using information on X and Y components.

Upon observation, it is evident that the best classification method is Random Forest, achieving a global accuracy of 61% with an IC 95% of [54%-68%] (recall=55%, AUC-ROC= 63%). A significant improvement of 8% was achieved in the representation of the X coordinate compared to the Y coordinate. This is primarily due to the fact that the main gait movements occur horizontally, leading to greater variances between joints in this orientation. It is important to note that the variance in joint movement during gait is expected to be cyclical, the abnormal fluctuations being an indicative of poor coordination. Secondly, covariance descriptor was coded from correlation between frame poses along video sequence (size of 70×70) to obtain a Parkinson classification. Table 2 summarizes achieved results, obtaining a general improvement in terms of accuracy values for several machine learning classifiers, including an

IC of 95%. In such cases, the results are associated with the capability of covariative descriptors to detect changes in speed, and postural configurations associated with Parkinson abnormalities.

Table 1. Comparative performance in different machine learning classification methods, using joints comparison (17 x 17 covariance matrices) for horizontal and vertical position. Source: own elaboration.

Method	X-position [IC 95%]			Y-position [IC 95%]		
	Accuracy	Recall	AUC-ROC	Accuracy	Recall	AUC-ROC
GB	0.56 [0.49-0.62]	0.49 [0.40-0.58]	0.59 [0.49-0.69]	0.53 [0.45-0.61]	0.43 [0.30-0.56]	0.55 [0.43-0.66]
NBY	0.16 [0.10-0.21]	0.21 [0.11-0.31]	0.08 [0.04-0.14]	0.56 [0.45-0.68]	0.16 [0.06-0.25]	0.64 [0.51-0.76]
KNN	0.55 [0.47-0.65]	0.33 [0.23-0.43]	0.58 [0.49-0.67]	0.57 [0.49-0.66]	0.40 [0.31-0.49]	0.54 [0.45-0.63]
SVM	0.47 [0.38-0.56]	0.22 [0.12-0.31]	0.39 [0.29-0.49]	0.57 [0.49-0.66]	0.31 [0.21-0.40]	0.58 [0.47-0.68]
RF	0.61 [0.54-0.68]	0.55 [0.47-0.64]	0.63 [0.54-0.72]	0.53 [0.44-0.62]	0.45 [0.33-0.58]	0.53 [0.41-0.66]

Table 2. Comparative performance from different machine learning classification methods, using frames and poses comparison (70 x 70 covariance matrices) for horizontal and vertical position, with IC 95%. Source: own elaboration.

Method	X-position [IC 95%]			Y-position [IC 95%]		
	Accuracy	Recall	AUC-ROC	Accuracy	Recall	AUC-ROC
GB	0.68 [0.60-0.78]	0.71 [0.59-0.84]	0.73 [0.62-0.85]	0.68 [0.59-0.77]	0.68 [0.54-0.81]	0.74 [0.62-0.87]
NBY	0.71 [0.61-0.80]	0.68 [0.55-0.80]	0.75 [0.63-0.86]	0.76 [0.66-0.86]	0.63 [0.47-0.79]	0.77 [0.67-0.87]
KNN	0.56 [0.47-0.64]	0.41 [0.29-0.53]	0.57 [0.46-0.67]	0.69 [0.61-0.78]	0.66 [0.54-0.79]	0.74 [0.63-0.86]
SVM	0.69 [0.61-0.79]	0.68 [0.56-0.82]	0.71 [0.60-0.85]	0.75 [0.65-0.85]	0.58 [0.41-0.75]	0.80 [0.68-0.92]
RF	0.72 [0.62-0.81]	0.75 [0.62-0.88]	0.73 [0.60-0.87]	0.72 [0.64-0.80]	0.71 [0.59-0.84]	0.77 [0.66-0.90]

Then, a spectral analysis was carried out in an additional experiment, considering a component reduction of covariance descriptors. In such a case, we only consider reduced covariances, reconstructed from principal eigenvectors. These experiments were carried out in covariances from correlations among postural changes along the video. In Table 3 the results are reported from compact covariances. A slight improvement in the value of the accuracy and AUC-ROC when a value of 20 elements was applied on the X-position with values of 71% and 70%, respectively. While for the Y-position many similar values are shown, generally in many of the reductions, reaching a maximum accuracy of 75% and AUC-ROC of 74% for 20, 30 and 40 values.

Table 3. Performance on 70x70 with Random Forest Classifier and reduced matrices using different quantities of values (10, 20, 30, 40, 50, 60) in horizontal and vertical position. Source: own elaboration.

Method	X-position		Y-position	
	Accuracy	AUC-ROC	Accuracy	AUC-ROC
No R	0.69	0.69	0.73	0.73
60	0.67	0.67	0.74	0.74
50	0.69	0.69	0.75	0.74
40	0.69	0.69	0.73	0.73
30	0.70	0.70	0.75	0.74
20	0.71	0.70	0.74	0.74
10	0.68	0.67	0.74	0.74

An observational analysis of disposed covariance descriptors was also performed to find localized differences between Parkinson and control patients. In Figure 3, we can observe different examples for patients with Parkinson's disease and control subjects.

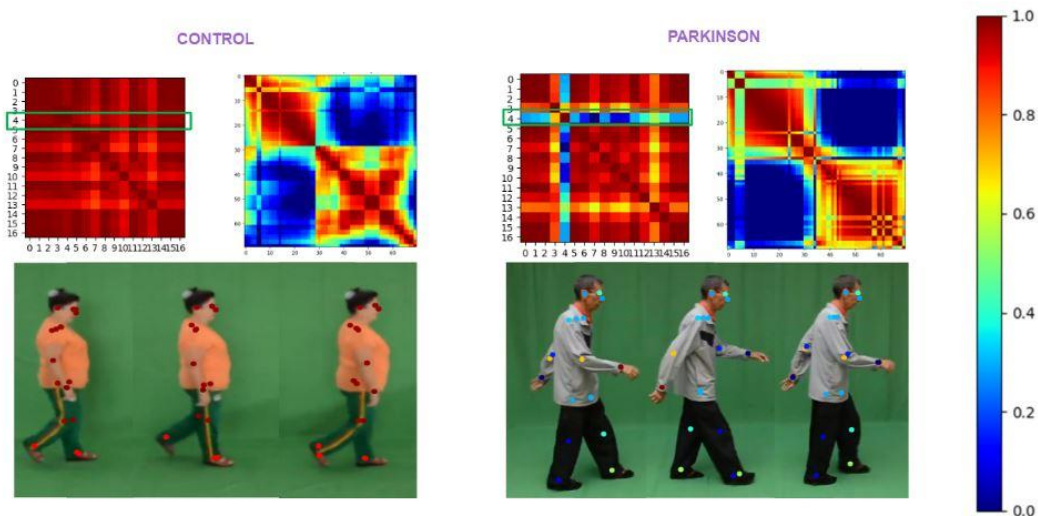


Figure 3. Correlation Matrix 17x17, showing the coordination of each landmark with the others and 70x70 joints analysis, showing the relation of the posture during each frame and gait cycles.

Source: own elaboration.

In this visualization, shades of blue indicate low correlation, while shades of red indicate strong correlation or dynamic coordination between the joints of interest. It is noteworthy that patients with Parkinson's disease exhibit low coordination values for the joint corresponding to the right hand (point 4) with the rest of the joints that are more coordinated, highlighting typical Parkinsonian patterns. The same process was applied to the 70x70 matrices, where each cell of the matrix represents the covariance between one frame and another, and each number corresponds to the analyzed frame number. In these matrices, correlated movements across several consecutive frames can be observed in control patients. However, in the case of Parkinson's patients, fluctuations in correlation values are evident, leading to an instability in the organization of their gait movements, Parkinson patients had more near to 0 values in correlation with these blue values. These patterns are clearly discernible in Figure 3 in the right matrix for each case.

4. DISCUSSION

Recent research aims to quantify Parkinson's motor patterns without physical markers or invasive setups [34], [35]. Several studies propose markerless video descriptors to approximate gait kinematics and classify motor patterns [24], [34], [35]. Deep learning on raw video inputs has achieved 88% accuracy on a dataset of 22 subjects [24]. In addition, a gait classification method based on limb-specific features reached 92.5% accuracy on a dataset of 40 patients, although it lacks full-body representation, which limits joint-level gait analysis [36]. This is a key aspect for clinical adoption, as Parkinson's assessment is based on localized kinematic analysis. Furthermore, a computer vision approach using region-based convolutional masks and a one-class SVM achieved 97.33% accuracy on a dataset of 114 healthy and 73 Parkinson's videos. However, classification was performed per video rather than per patient [37]. Similarly, a pose-based human action recognition framework using spatio-temporal descriptors encoded with Fisher vectors and hybrid kernel models obtained accuracies of 89% and 97%, although the method struggled to distinguish identical poses in different actions [38]. Moreover, a

markerless gait analysis method that projects videos into deep feature representations and encodes them as compact covariance matrices on a Riemannian manifold achieved 99% accuracy by leveraging geometric means and principal geodesic directions for classification. However, full video analysis may introduce background artifacts that affect the results [39]. In contrast, gait analysis based on vertical ground reaction force (VGRF) data achieved up to 98.4% accuracy using KNN, Naive Bayes, ensemble classifiers, and SVM. Despite the high performance, this approach is invasive and limited to foot analysis [40].

Despite the remarkable results of these approaches, the coarse classification remains far from standard clinical practice, limiting their applicability in real scenarios. For instance, physicians are interested in observing and explaining abnormal behaviors that occur between joints, which are supported by medical literature. In this line, the proposed approach emulates a standard gait analysis by computing markerless postures at each frame, allowing the kinematics of each joint for lower and upper limbs to be taken as reference. Thus, the proposed approach computes coordination variables and compact second-order statistics, which may be explainable for Parkinson's automatic classification. In contrast, although the proposed approach follows a markerless framework, it preserves local joint analysis by retrieving postures during locomotion observation. In this sense, the output of the Parkinson predictions can be reversed to obtain the correlation between joints that may support the Parkinson/healthy label.

This point is fundamental for mapping the approach into clinical routines, as it is easily adaptable to standard motor scales. The proposed approach, evaluated on a study with 30 recorded patients, achieved an average accuracy and recall of 75% and 75%, respectively, complementing an AUC-ROC of 74%. In addition, two different analyses were conducted to explain major incidences from postural and joint perspectives. Nevertheless, the dataset employed is constrained to the sagittal plane of gait, which may constitute a limitation of the proposed method. Specifically, certain inter-joint relationships and positional data could be affected by occlusions or inaccuracies inherent to the pose estimation process, potentially leading to deviations from the actual gait patterns of the analyzed subjects. Moreover, the relatively small dataset size represents an additional limitation, as it is currently under construction and being expanded as part of an ongoing effort by our research group. Furthermore, our covariance-based analysis methodology still presents certain limitations, as it heavily relies on positional features, which, while significant, may not fully capture all relevant patterns associated with Parkinson's disease. The study presented in this work achieves correspondences in the sagittal plane but has limitations in capturing volumetric orientations of body segments that may reflect segmental variations during gait. This constraint arises from the absence of 3D information required to perform such calculations. Therefore, future studies could explore the detection of rotational alignment of segments within a volumetric environment. Additionally, future studies should consider the normalization and standardization of subjects according to anthropometric variables to ensure more comparable and generalizable results.

5. CONCLUDING REMARKS

This work introduced a methodology centered on gait characterization using covariance matrices. This approach allows the discrimination between individuals diagnosed with Parkinson's disease (PD) and control subjects. Posture-based representations were derived using the OpenPose architecture, providing posture-related information to carry out classification tasks. The results indicate that using covariance matrices extracted from poses in each frame leads to improved classification metrics. In the clinical domain, these analyses are particularly relevant for identifying factors associated with movement coordination during gait, as they enable the examination of positional relationships among joints over time within a controlled clinical environment. Such analyses can contribute to rehabilitation and treatment

processes for Parkinson's disease by helping clinicians focus on specific phases or regions of the gait cycle that require targeted intervention.

Notably, reducing the dimensionality of these matrices using eigenvectors and eigenvalues resulted in a slight performance enhancement. Despite these advancements, our approach still has limitations. It heavily relies on positional features, which, while significant, may not fully capture all relevant patterns associated with Parkinson's disease. Expanding the feature set could enhance the analysis, offering a more comprehensive understanding of the disease. Additionally, future studies would benefit from a larger, more recent dataset, enabling different perspectives of gait execution, even more robust comparisons and validations of our findings.

6. ACKNOWLEDGMENTS

We express our gratitude to the Biomedical Imaging, Vision, and Learning Laboratory (BIVL²ab) and its members for their support in the development of this project, providing necessary materials and guidance for its execution, as well as for their valuable input on the manuscript. We also thank the School of Physical Therapy at UIS for their insightful recommendations on understanding Parkinson's disease and locomotion patterns. Our appreciation extends to FAMPAS and FOSCAL for their collaboration in developing the database used in this study. Finally, we acknowledge the Ministry of Science, Technology, and Innovation of Colombia for supporting this research through the project "Caracterización de movimientos anormales del Parkinson desde patrones oculomotores, de marcha y enfoques multimodales basados en visión computacional" (Project Code: 92694).

7. REFERENCES

- [1] GBD 2017 US Neurological Disorders Collaborators, "Burden of Neurological Disorders Across the US From 1990-2017: A Global Burden of Disease Study," *JAMA Neurol.*, vol. 78, no. 2, pp. 165-176, Feb. 2021. <https://doi.org/10.1001/jamaneurol.2020.4152>
- [2] A. Zhao, E. Cui, A. Leroux, M. A. Lindquist, and C. M. Crainiceanu, "Evaluating the prediction performance of objective physical activity measures for incident Parkinson's disease in the UK Biobank," *J. Neurol.*, vol. 270, no. 12, pp. 5913-5923, Aug. 2023. <https://doi.org/10.1007/s00415-023-11939-0>
- [3] E. Ray Dorsey, T. Sherer, M. S. Okun, and B. R. Bloem, "The Emerging Evidence of the Parkinson Pandemic," *J. Park. Dis.*, vol. 8, no. s1, pp. S3-S8, Dec. 2018. <https://doi.org/10.3233/JPD-181474>
- [4] E. Rovini, C. Maremmani, and F. Cavallo, "How Wearable Sensors Can Support Parkinson's Disease Diagnosis and Treatment: A Systematic Review," *Front. Neurosci.*, vol. 11, Oct. 2017. <https://doi.org/10.3389/fnins.2017.00555>
- [5] R. Baker, "Gait analysis methods in rehabilitation," *J. NeuroEngineering Rehabil.*, vol. 3, no. 4, Mar. 2006. <https://doi.org/10.1186/1743-0003-3-4>
- [6] J. Kulisevsky et al., "Enfermedad de Parkinson avanzada. Características clínicas y tratamiento (parte I)," *Neurología*, vol. 28, no. 8, pp. 503-521, Oct. 2013. <https://doi.org/10.1016/j.nrl.2013.05.001>
- [7] W. Poewe et al., "Parkinson disease," *Nat. Rev. Dis. Primer*, vol. 3, no. 1, pp. 1-21, Mar. 2017. <https://doi.org/10.1038/nrdp.2017.13>
- [8] K. Berganzo et al., "Motor and non-motor symptoms of Parkinson's disease and their impact on quality of life and on different clinical subgroups," *Neurol. Engl. Ed.*, vol. 31, no. 9, pp. 585-591, Nov.-Dec. 2016. <https://doi.org/10.1016/j.nrleng.2014.10.016>
- [9] C. León-Jiménez, "Síndrome rígido acinético," *Rev. Med. Clínica*, vol. 3, no. 2, pp. 104-108, May. 2019. <https://doi.org/10.5281/ZENODO.3236571>

- [10] N. B. Ramírez, N. P. Álvarez, S. Q. Aguilar, and L. N. Orozco, "Datos clave para el diagnóstico clínico de enfermedad de Parkinson," *Rev. Mex. Neurocienc.*, vol. 10, no. 5, pp. 340-343, Sep.-Oct. 2009. <https://www.medigraphic.com/cgi-bin/new/resumen.cgi?IDARTICULO=44661>
- [11] S. Garrido-Elustondo, B. Reneses, A. Navalón, O. Martín, I. Ramos, and M. Fuentes, "Capacidad de detección de patología psiquiátrica por el médico de familia," *Aten. Primaria*, vol. 48, no. 7, pp. 449-457, Aug.-Sep. 2016. <https://doi.org/10.1016/j.aprim.2015.09.009>
- [12] M. Iosa, P. Picerno, S. Paolucci, and G. Morone, "Wearable inertial sensors for human movement analysis," *Expert Rev. Med. Devices*, vol. 13, no. 7, pp. 641-659, Jun. 2016. <https://doi.org/10.1080/17434440.2016.1198694>
- [13] The Lancet, "Artificial intelligence in health care: within touching distance," *Lancet Lond. Engl.*, vol. 390, no. 10114, p. 2739, Dec. 2017. [https://doi.org/10.1016/S0140-6736\(17\)31540-4](https://doi.org/10.1016/S0140-6736(17)31540-4)
- [14] R. Caldas, M. Mundt, W. Potthast, F. Buarque de Lima Neto, and B. Markert, "A systematic review of gait analysis methods based on inertial sensors and adaptive algorithms," *Gait Posture*, vol. 57, pp. 204-210, Sep. 2017. <https://doi.org/10.1016/j.gaitpost.2017.06.019>
- [15] G. Pal, and C. G. Goetz, "Assessing Bradykinesia in Parkinsonian Disorders," *Front. Neurol.*, vol. 4, Jun. 2013. <https://doi.org/10.3389/fneur.2013.00054>
- [16] C.-Y. Hsu, Y.-S. Tsai, C.-S. Yau, H.-H. Shie, and C.-M. Wu, "Test-Retest Reliability of an Automated Infrared-Assisted Trunk Accelerometer-Based Gait Analysis System," *Sensors*, vol. 16, no. 8, p. 1156, Aug. 2016. <https://doi.org/10.3390/s16081156>
- [17] E. Balaji, D. Brindha, and R. Balakrishnan, "Supervised machine learning based gait classification system for early detection and stage classification of Parkinson's disease," *Appl. Soft Comput.*, vol. 94, p. 106494, Sep. 2020. <https://doi.org/10.1016/j.asoc.2020.106494>
- [18] A. I. Cuesta-Vargas, A. Galán-Mercant, and J. M. Williams, "The use of inertial sensors system for human motion analysis," *Phys. Ther. Rev.*, vol. 15, no. 6, pp. 462-473, Dec. 2010. <https://doi.org/10.1179/1743288X11Y.0000000006>
- [19] C. Wong, Z.-Q. Zhang, B. Lo, and G.-Z. Yang, "Wearable Sensing for Solid Biomechanics: A Review," *IEEE Sens. J.*, vol. 15, no. 5, pp. 2747-2760, May. 2015. <https://doi.org/10.1109/JSEN.2015.2393883>
- [20] C.-W. Cho, W.-H. Chao, S.-H. Lin, and Y.-Y. Chen, "A vision-based analysis system for gait recognition in patients with Parkinson's disease," *Expert Syst. Appl.*, vol. 36, no. 3, Part 2, pp. 7033-7039, Apr. 2009. <https://doi.org/10.1016/j.eswa.2008.08.076>
- [21] O. Ćupa et al., "Motion tracking and gait feature estimation for recognising Parkinson's disease using MS Kinect," *Biomed. Eng. OnLine*, vol. 14, no. 97, Oct. 2015. <https://doi.org/10.1186/s12938-015-0092-7>
- [22] A. Viswakumar, V. Rajagopalan, T. Ray, and C. Parimi, "Human Gait Analysis Using OpenPose," in *2019 Fifth Int. Conf. Image Inform. Process. (ICIIP)*, Shimla, India, 2019, pp. 310-314. <https://doi.org/10.1109/ICIIP47207.2019.8985781>
- [23] A. Rohan, M. Rabah, T. Hosny, and S.-H. Kim, "Human Pose Estimation-Based Real-Time Gait Analysis Using Convolutional Neural Network," *IEEE Access*, vol. 8, pp. 191542-191550, 2020. <https://doi.org/10.1109/ACCESS.2020.3030086>
- [24] L. C. Guayacán, and F. Martínez, "Visualising and quantifying relevant parkinsonian gait patterns using 3D convolutional network," *J. Biomed. Inform.*, vol. 123, p. 103935, Nov. 2021. <https://doi.org/10.1016/j.jbi.2021.103935>
- [25] G. Varol, I. Laptev, and C. Schmid, "Long-Term Temporal Convolutions for Action Recognition," *IEEE Trans. Pattern Anal. Mach. Intell.*, vol. 40, no. 6, pp. 1510-1517, Jun. 2018. <https://doi.org/10.1109/TPAMI.2017.2712608>
- [26] Z. Cao, T. Simon, S.-E. Wei, and Y. Sheikh, "Realtime Multi-Person 2D Pose Estimation Using Part Affinity Fields," in *Proceed. IEEE Conf. Comput. Vision Pattern Recogn.*, 2017, pp. 7291-7299. <https://doi.org/10.48550/arXiv.1611.08050>

- [27] R. Bhidayasiri, and D. Tarsy, "Parkinson's Disease: Hoehn and Yahr Scale," in *Movement Disorders: A Video Atlas: A Video Atlas*, R. Bhidayasiri, and D. Tarsy, Eds., Totowa, NJ: Humana Press, 2012, pp. 4-5. https://doi.org/10.1007/978-1-60327-426-5_2
- [28] R. Moe-Nilssen, M. K. Aaslund, C. Hodt-Billington, and J. L. Helbostad, "Gait variability measures may represent different constructs," *Gait Posture*, vol. 32, no. 1, pp. 98-101, May. 2010. <https://doi.org/10.1016/j.gaitpost.2010.03.019>
- [29] A. Kale, N. Cuntoor, B. Yegnanarayana, A. N. Rajagopalan, and R. Chellappa, "Gait Analysis for Human Identification," in *Audio- and Video-Based Biometric Person Authentication*, J. Kittler, and M. S. Nixon, Eds., Berlin, Heidelberg: Springer, 2003, pp. 706-714. https://doi.org/10.1007/3-540-44887-X_82
- [30] Y. Liu, Y. Wang, and J. Zhang, "New Machine Learning Algorithm: Random Forest," en *Information Computing and Applications*, B. Liu, M. Ma, and J. Chang, Eds., Berlin, Heidelberg: Springer, 2012, pp. 246-252. https://doi.org/10.1007/978-3-642-34062-8_32
- [31] Z. Zhang, "Introduction to machine learning: k-nearest neighbors," *Ann. Transl. Med.*, vol. 4, no. 11, p. 218, Jun. 2016. <https://doi.org/10.21037/atm.2016.03.37>
- [32] H. Zhang, and J. Su, "Naive Bayesian Classifiers for Ranking," in *Machine Learning: ECML 2004*, J.-F. Boulicaut, F. Esposito, F. Giannotti, and D. Pedreschi, Eds., Berlin, Heidelberg: Springer, 2004, pp. 501-512. https://doi.org/10.1007/978-3-540-30115-8_46
- [33] C. Bentéjac, A. Csörgő, and G. Martínez-Muñoz, "A comparative analysis of gradient boosting algorithms", *Artif. Intell. Rev.*, vol. 54, no. 3, pp. 1937-1967, Mar. 2021. <https://doi.org/10.1007/s10462-020-09896-5>
- [34] N. Kour, S. Gupta, and S. Arora, "Computer-Vision Based Diagnosis of Parkinson's Disease via Gait: A Survey," *IEEE Access*, vol. 7, pp. 156620-156645, Oct. 2019. <https://doi.org/10.1109/ACCESS.2019.2949744>
- [35] A. Landolfi et al., "Machine Learning Approaches in Parkinson's Disease", *Curr. Med. Chem.*, vol. 28, no. 32, pp. 6548-6568, Oct. 2021. <https://doi.org/10.2174/092986732899921011211420>
- [36] Y. Yang, P. Liu, Y. Sun, N. Yu, J. Wu, and J. Han, "A Video-Based Method to Classify Abnormal Gait for Remote Screening of Parkinson's Disease," in *2021 40th Chinese Control Conf. (CCC)*, Shanghai, China, 2021, pp. 3357-3362. <https://doi.org/10.23919/CCC52363.2021.9549992>
- [37] L. Gong, J. Li, M. Yu, M. Zhu, and R. Clifford, "A novel computer vision based gait analysis technique for normal and Parkinson's gaits classification," in *2020 IEEE Int. Conf. Dependable Autonomic Secure Computing, Intl Conf on Pervasive Intelligence and Computing*, Calgary, AB, Canada, 2020, pp. 209-215. <https://doi.org/10.1109/DASC-PICom-CBDCom-CyberSciTech49142.2020.00045>
- [38] S. Agahian, F. Negin, and C. Köse, "An efficient human action recognition framework with pose-based spatiotemporal features," *Eng. Sci. Technol. Int. J.*, vol. 23, no. 1, pp. 196-203, Feb. 2020. <https://doi.org/10.1016/j.jestch.2019.04.014>
- [39] S. Niño, J. A. Olmos, J. C. Galvis, and F. Martínez, "Parkinsonian gait patterns quantification from principal geodesic analysis," *Pattern Anal. Appl.*, vol. 26, no. 2, pp. 679-689, May. 2023. <https://doi.org/10.1007/s10044-022-01115-x>
- [40] E. Balaji, D. Brindha, V. K. Elumalai, and K. Umesh, "Data-driven gait analysis for diagnosis and severity rating of Parkinson's disease," *Med. Eng. Phys.*, vol. 91, no. 1, pp. 54-64, May. 2021. <https://doi.org/10.1016/j.medengphy.2021.03.005>

CONFLICT OF INTEREST

The authors declare that they have no conflict of interest.

AUTHORSHIP CONTRIBUTION

Jean Portilla: Methodology, Software, Visualization, discussion, Validation, Data analysis, Data acquisition.

Edgar Rangel Pieschacon: Data curation, Visualization, discussion, Validation.

Odair Bacca: Data acquisition, Data analysis, Validation, discussion.

Paula C. Ramírez: Data acquisition, Data analysis, Validation, discussion.

Luis Guayacán: Data curation, Visualization, discussion, Validation.

Fabio Martínez Carrillo: Investigation, Conceptualization, Methodology, Supervision, discussion, Validation, Data analysis, Funding acquisition, Resources.

All authors were involved in the Writing-Reviewing and Editing process.